HHS Public Access

Author manuscript

J Membr Biol. Author manuscript; available in PMC 2015 November 06.

Published in final edited form as:

J Membr Biol. 2012 March ; 245(3): 131–140. doi:10.1007/s00232-012-9421-y.

Effect of Simultaneously Replacing Putative TM6 and TM12 of Human NBCe1-A with Those from NBCn1 on Surface Abundance in *Xenopus* Oocytes

Li-Ming Chen,
Department of Biological Sciences, Key Laboratory of Molecular Biophysics of the Ministry of Education, College of Life Science and Technology, Huazhong University of Science & Technology, Wuhan 430074, Hubei Province, China

Xue Qin,
Department of Physiology and Biophysics, Case Western Reserve University School of Medicine, 10900 Euclid Avenue, Cleveland, OH 44106, USA

Fraser J. Moss,
Department of Physiology and Biophysics, Case Western Reserve University School of Medicine, 10900 Euclid Avenue, Cleveland, OH 44106, USA

Ying Liu, and
Department of Biological Sciences, Key Laboratory of Molecular Biophysics of the Ministry of Education, College of Life Science and Technology, Huazhong University of Science & Technology, Wuhan 430074, Hubei Province, China

Walter F. Boron
Department of Physiology and Biophysics, Case Western Reserve University School of Medicine, 10900 Euclid Avenue, Cleveland, OH 44106, USA

Li-Ming Chen: liming.chen@mail.hust.edu.cn; Walter F. Boron: walter.boron@case.edu

Abstract

HCO_3^- translocation across the plasma membrane via the electrogenic Na/HCO_3^- cotransporter NBCe1 plays an important role in intracellular pH regulation and transepithelial HCO_3^- transport. However, the structural determinants of transporter function remain largely unknown. A previous study showed that the putative fourth extracellular loop (EL4) plays an essential role in determining the electrogenicity of NBCe1. In the present study, we generated eight new chimeras of human NBCe1-A and NBCn1-A. All possess the putative NBCe1 EL4 and are electrogenic. Chimera O, in which the putative sixth transmembrane segment (TM6) and EL5 through the C terminus (Ct) of NBCe1 was replaced by corresponding NBCn1 sequence, produces the smallest hyperpolarization (1–2 mV) when CO_2/HCO_3^- is added to the extracellular solution. Biotinylation experiments show that O has a very low abundance at the plasma membrane. However, chimeras in which we simultaneously replaced the putative TM6 and smaller subdomains of the EL5-Ct region for the NBCn1 sequence were strongly electrogenic except for chimera T, in which we

Correspondence to: Li-Ming Chen, liming.chen@mail.hust.edu.cn; Walter F. Boron, walter.boron@case.edu.
Xue Qin and Fraser J. Moss contributed equally to this work.

replaced TM6 and TM12 of NBCe1 with the corresponding regions of NBCn1. T exhibited greatly reduced transporter surface expression compared to wild-type NBCe1-A, while retaining at least some electrogenic character. We hypothesize that putative TM6 and TM12 are part of a functional unit and that if the two TMs are replaced by those of the same transporter type, high surface expression would require that the surrounding TMs are also from the same transporter type.

Keywords

Xenopus oocyte; SLC4A4; SLC4A7; Intracellular pH; Biotinylation; Bicarbonate transporter

Introduction

For secondary active transport, substrate stoichiometry is a fundamentally important property. Among the five Na-coupled HCO_3^- transporters (NCBTs) of the SLC4 family, differences in stoichiometry cause them to fall into two groups based on net charge movement: (1) the electrogenic Na/HCO_3 cotransporters NBCe1 (Romero et al. 1997) and NBCe2 (Virkki et al. 2002; Sassani et al. 2002) and (2) the electroneutral NCBTs, which include NBCn1 (Choi et al. 2000; Pushkin et al. 1999) and NBCn2 (aka NCBE, see Parker et al. 2008; Wang et al. 2000) as well as the Na^+-driven $Cl\text{-}HCO_3^-$ exchanger NDCBE (Grichtchenko et al. 2001). On the one hand, electrogenic transport can have profound effects on the membrane potential (V_m) and, thus, could affect a wide range of voltage-sensitive biological processes, such as gating of and flux through ion channels. On the other hand, the electrogenicity (or lack thereof) impacts the thermodynamics of the transporter even to the extent that it can determine the direction of net transport.

The electrogenic NBCe1 and electroneutral NBCn1 have broad physiological relevance. Mutations in NBCe1 have been associated with proximal renal tubular acidosis, mental retardation as well as ocular and dental defects (for review, see Boron et al. 2009). A carboxyl-terminally truncated NBCe1 mutant with impaired trafficking to the plasma membrane is associated with hemiplegic migraine (Suzuki et al. 2010). Targeted disruption of *Slc4a4* in mice severely impairs the formation of dental enamel, indicating that NBCe1 is essential for normal development of dentition (Lacruz et al. 2010). The complex expression and distribution of at least five NBCe1 variants in the reproductive tract tissues suggest that the transporter plays important roles in mammalian reproduction (Liu et al. 2011).

NBCn1 appears to be important in both normal physiology and pathophysiology. In osteoclasts, NBCn1 is responsible for the increase in intracellular pH (pH_i) triggered by colony-stimulating factor 1, resulting in enhanced cell survival (Bouyer et al. 2007). NBCn1 is also necessary for the degradation of hydroxyapatite by osteoclasts (Riihonen et al. 2010). Polymorphisms in NBCn1 are associated with an increase in susceptibility to breast cancer (Antoniou et al. 2010; Ahmed et al. 2009). Moreover, in a human breast-cancer cell line, NBCn1 abundance is substantially enhanced by the expression of a constitutively active, truncated receptor tyrosine kinase, ErbB2, that is commonly expressed in breast cancer (Lauritzen et al. 2010). In addition, knockout of NBCn1 in mice is associated with blindness and deafness (Bok et al. 2003). Boedtkjer et al. (2011) have shown that NO-mediated

vasorelaxation as well as hypertension development are inhibited in NBCn1-null mice. Moreover, a genomewide association study has shown that variations in *SLC4A7* are associated with hypertension and increased cardiovascular disease risk in humans (Ehret et al. 2011). Finally, allelic variants of *SLC4A7* could contribute to the vulnerability to drug addiction (Ishiguro et al. 2007).

Interestingly, the electrogenic NBCe1 and electroneutral NBCn1 appear to have opposite roles in the heart. Inhibition of NBCe1 reduces ischemic injury in rat cardiac myocytes (Khandoudi et al. 2001). In contrast, knock-down of NBCn1 increases ischemia-induced apoptosis of coronary endothelial cells (Kumar et al. 2010). This last observation, which is consistent with an antiapoptotic effect of NBCn1, is in harmony with the aforementioned osteoclast data. De Giusti et al. (2009) demonstrated that angiotensin II stimulates Na-coupled HCO_3^- transport and presumably electroneutral NBC activity in cardiac myocytes. On the other hand, the same group showed that angiotensin II inhibits electrogenic Na-coupled HCO_3^- transport in cardiac myocytes (De Giusti et al. 2010).

Given the physiological significance of NBCe1 and NBCn1, it is important to understand the molecular mechanism of ion transport by these two transporters. Based upon a study with AE1 (Zhu et al. 2003), Romero et al. (2004) proposed that all SLC4 family members consist of a large soluble cytosolic N-terminal domain (Nt), followed by a transmembrane domain (TMD) containing 14 transmembrane segments (TMs), including 13 helices and one reentrant loop connecting the extracellular end of TM11 and the intracellular end of TM13, and a short cytosolic C-terminal domain (Ct). The putative large third extracellular loop (EL3) between TM5 and TM6 divides the TMD into two parts, the front half (TMD_F) consisting of TM1–TM5 and the back half (TMD_B) consisting of TM6–TM14. Choi et al. (2007) demonstrated that the electrogenicity of rat NBCe1 requires the simultaneous presence of TMD_F and TMD_B. Chen et al. (2011) later demonstrated that the putative fourth extracellular loop (EL4) plays a critical role in determining the electrogenicity vs. electroneutrality of human NBCe1-n1 chimeras. Simply replacing EL4 of NBCe1 with that of NBCn1 (construct M in that study) virtually eliminated electrogenicity, while retaining substantial HCO_3^- transport activity. Moreover, the reverse replacement engendered electrogenicity in an electroneutral chimera.

In the present study, we generated eight new NBCe1-n1 chimeras in the TMD_B, all of which contained the EL4 of NBCe1. We demonstrate that all chimeras are electrogenic. However, the simultaneous replacement of TM6 and TM12 of NBCe1-A with those from NBCn1—but not the simultaneous replacements of TM6 with EL5, TM10, TM11, TM13 or TM14—greatly reduced the surface expression of the chimera when expressed in *Xenopus* oocytes. We hypothesize that TM6 and TM12 are part of a functional unit and that, when they are replaced together, normal surface expression requires that the surrounding TMs be from the same transporter type.

Methods

Construct, Oocyte Injection and Electrophysiologic Measurements

As previously described (Chen et al. 2011), chimeras were generated by polymerase chain reaction using human NBCe1-A (accession NM_003759) and human NBCn1-A (accession AF047033) as templates. All constructs were tagged at amino termini with enhanced green fluorescent protein (EGFP). Although it is possible that this tag could have influenced our results, a comparison with historical transport rates suggests that the Nt-EGFP tag did not reduce activity. In the data set for our previous study (Chen et al. 2011), construct A had a mean slope conductance of ~ 35 μS in 5% CO_2/33 mM HCO_3^- (not previously published), which is modestly higher than the value of ~24 μS observed under similar conditions with untagged rat NBCe1-A (Choi et al. 2007).

Figure 1 shows the putative topology—proposed by Romero et al. (2004) based on the AE1 model of Zhu et al. (2003)—and sequence boundaries for all constructs that we used in the present study. For the convenience of readers, each construct is designated an alphabetical code consistent with that of our previous article (Chen et al. 2011). The construct cDNAs were linearized by restriction digestion with *Not*I for cRNA synthesis. cRNA was transcribed with T7 RNA polymerase using the mMessage mMachine kit (Ambion, Austin, TX) and stored at −80°C until injected.

In most cases, we obtained *Xenopus laevis* oocytes from an ovarian lobe following a protocol approved by the Institutional Animal Care and Use Committee at Case Western Reserve University. In some cases, we purchased ovaries from NASCO (Fort Atkinson, WI). Each oocyte was injected with 50 nl of cRNA (0.5 μg/μl), encoding a transporter or 50 nl H_2O as a control, and incubated at 18°C for 4–5 days until used for assay.

For 4,4-diisothiocyanatostilbene-2,2-disulfonic acid (DIDS) experiments, we used a nominally CO_2/HCO_3^--free ND96 solution that contained in (mM) 93.5 NaCl, 2 KCl, 1 $MgCl_2$, 1.8 $CaCl_2$ and 5 HEPES. DIDS-containing solutions (400 μM) were made freshly by adding DIDS powder to ND96 or 1.5% CO_2. A 0.2% BSA solution was made freshly by adding albumin powder (0.2 g/100 ml) to ND96 or 1.5% CO_2. Preparation of all other solutions as well as the measurements of V_m and pH_i were performed as previously described (Chen et al. 2011).

Examination of Total and Membrane Proteins Expressed in *Xenopus* Oocytes

For the detection of transporter proteins expressed at the plasma membrane, we biotinylated and then isolated proteins on the extracellular surface of *Xenopus* oocytes using the Pinpoint™ Cell Surface Protein Isolation Kit (catalog 89881; Pierce, Rockford, IL), modifying the manufacturer's protocol for use with oocytes. For each group, 15 oocytes were washed with ice-cold phosphate-buffered saline (PBS, diluted to ~200 mOsm) and incubated in 5 ml PBS containing 1.2 mg Sulfo-NHS-SS-Biotin on a rocker for 1 h at 4°C. The reaction was stopped by adding 250 μl quenching solution. Oocytes were next washed in TRIS-buffered saline (TBS, diluted to ~200 mOsm) for 5 min, then homogenized with a pellet pestle (Kimble Chase Kontes, Vineland, NJ) in 450 μl lysis buffer, which consisted of 1% Triton X-100 (Sigma-Aldrich, St. Louis, MO) and one tablet EDTA-free proteinase

inhibitors (Roche Diagnostics, Indianapolis, IN) per 10 ml of TBS. Lysates were centrifuged for 10 min at 1,000×*g* and 4°C. The lipid layer on the top of the supernatant was carefully removed. Some of the supernatant was withheld at this stage and used to assay the amount of total protein fraction. The remaining material was incubated with 500 μl Immobilized Neutravidin™ Gel (Pierce) and incubated for 1 h at room temperature. After five washes with 500 μl lysis buffer, biotinylated proteins were eluted by incubation for 1 h at room temperature in 1 × SDS polyacrylamide gel electrophoresis (SDS-PAGE) sample buffer containing 50 mM DTT. The resulting preparation represents the surface-protein fraction of *Xenopus* oocytes.

The total and surface-protein fractions were separated on SDS-PAGE and then transferred onto an Immobilon™ PVDF membrane (Millipore, Bedford, MA). The blot was probed with monoclonal mouse anti-EGFP primary antibody (Clontech, Palo Alto, CA) at 1:2,000 dilution and then with HRP-conjugated goat anti-mouse secondary antibody (MP Biomedicals, Solon, OH) at 1:5,000. Chemiluminescence was performed with the Amersham ECL Plus Western Blotting Detection Reagents (GE Healthcare, Aylesbury, UK) prior to X-ray film exposure.

Results

V_m and pH_i Measurements of Oocytes Expressing Transporters

Figure 2a shows typical V_m and pH_i records from an oocyte expressing wild-type (wt) human NBCe1-A (construct A). The oocyte was superfused with nominally HCO_3^--free ND96 solution and then with 1.5% CO_2/10 mM HCO_3^-. The addition of CO_2/HCO_3^- caused an abrupt hyperpolarization (V_m, red trace), a change characteristic of an electrogenic NBC. Moreover, after rapid CO_2-induced intracellular acidification, pH_i recovered robustly (green trace). The rate of pH_i recovery (dpHi/dt) reflects the rate of transporter-mediated uptake of HCO_3^- or a related ion (e.g., $CO_3^=$) and is thus an index of NBC activity. Note also that removing Na^+ from the extracellular solution produced the opposite set of changes: an instantaneous depolarization and a rapid fall in pH_i; the depolarization is indicative of electrogenic NBC activity. In the control oocyte injected with H_2O (Fig. 2b), the switch to CO_2/HCO_3^- failed to elicit either an instantaneous hyperpolarization or a pH_i recovery from the acid load.

As shown in our previous article (Chen et al. 2011), on the background of wt human NBCe1-A, replacing the fragment from the putative EL5 through the Ct, inclusive, with the corresponding region of human NBCn1-A resulted in an electrogenic chimera (construct G). Representative recordings of V_m and pH_i from an oocyte expressing construct G are shown in Fig. 3a.

On the background of construct G, we created the novel construct O by replacing TM6 of NBCe1 with TM6 of NBCn1. This manipulation had a severe effect on the functional expression. As shown in Fig. 3b, the oocyte expressing construct O exhibited virtually no pH_i recovery. The dominant effect on V_m was a sustained depolarization that was reminiscent of the H_2O-injected oocyte in Fig. 2b. However, closer examination of Fig. 3b reveals that the switch to CO_2/HCO_3^- caused a small transient hyperpolarization. Moreover,

we observed similar transient hyperpolarizations of 1–2 mV in each of the nine oocytes that we injected with cRNA encoding construct O and then later examined electrophysiologically. Thus, construct O has at least some electrogenic character.

On the background of wt human NBCe1-A, we created construct P by simply replacing TM6 of NBCe1 with TM6 of NBCn1. This construct retained obvious electrogenicity as well as robust HCO_3^--transport activity (Fig. 3c). Taken together, the data from Fig. 3 show that, although the replacement of only one of the two NBCe1 structural elements at a time (Fig. 3a, c) produces an electrogenic chimera that expresses robustly, the simultaneous replacement of the two structural elements together results in a chimera with at least some electrogenic character but extremely low functional expression in *Xenopus* oocytes.

The above observations are consistent with the hypothesis that putative TM6 interacts with a structural component between putative EL5 and Ct, inclusive. In order to define this latter structural element, we created a series of chimeras on the background of construct P by replacing single putative loops or TMs from EL5 through TM14 of NBCe1-A with the corresponding element of human NBCn1. As shown in Fig. 4a, construct Q, in which we simultaneously replaced putative TM6 and EL5 of NBCe1-A, retained electrogenicity and robust HCO_3^--transport activity. We made similar observations for construct R (Fig. 4b, putative TM6 and TM10) and construct S (Fig. 4c, putative TM6 and TM11). We did not swap the intervening putative intracellular loop 5, which is only three amino acids long.

Simultaneously replacing putative TM6 and TM12 of NBCe1-A to produce construct T virtually eliminated functional expression, as judged by the pH_i-recovery rate (Fig. 5a). However, construct T was not totally inactive because the switch to CO_2/HCO_3^- elicited a modest instantaneous hyperpolarization. On the other hand, construct U (Fig. 5b, TM6 and TM13-EL6) and construct V (Fig. 5c, TM6 and TM14) retained electrogenicity as well as substantial HCO_3^--transport activity.

Figure 6 summarizes the data on pH_i recovery rate and ΔV_m for CO_2/HCO_3^- exposure experiments like those shown in Figs. 2, 3, 4, and 5. Although very small, both the mean ΔV_m (-1.4 ± 0.2 mV) and the mean dpH_i/dt ($[3.0 \pm 0.3] \times 10^{-5}$ pH units/s) of oocytes expressing construct O were significantly different from those of H_2O-injected oocytes (-0.6 ± 0.2 mV, $P = 0.007$; $[1.0 \pm 0.4] \times 10^{-5}$ pH units/s, $P = 0.006$). For oocytes expressing construct T, the mean ΔV_m was -8.0 ± 0.7 mV, which was significantly greater than that of H_2O-injected oocytes ($P = 7.7 \times 10^{-5}$), although dpH_i/dt was not significantly different ($P = 0.16$). This discordance is not surprising inasmuch as, in oocytes, ΔV_m is the most sensitive indicator of electrogenic NBC activity. Thus, we conclude that construct T retains at least some electrogenic character but has low functional activity. Note that construct M from the previous study (Chen et al. 2011), which has a predominantly electroneutral character, had a far smaller ΔV_m (-3.6 mV) than T but a substantially greater dpH_i/dt (6.8×10^{-5} pH units/s).

Returning to Fig. 6, we see that both ΔV_m and dpH_i/dt of other groups are, of course, significantly different from those of H_2O-injected oocytes ($P < 0.001$ for all other cases).

Effects of DIDS on Construct O and T

A major feature of NBCe1 is the sensitivity to DIDS. The DIDS-binding motif KKMIK of NBCe1, thought to be near the extracellular end of putative TM5 (Lu and Boron 2007), is present in all chimeras. Because the ΔV_m values for constructs O and T were small, we assayed the inhibitory effect of DIDS (Fig. 7) to test the hypothesis that the small V_m changes were indeed mediated by NBCe1/n1 chimeras O and T and not by some conductance native to the oocyte.

Consistent with the result shown in Fig. 3b, exposing an oocyte expressing construct O to 1.5% CO_2/10 mM HCO_3^- caused a hyperpolarization of ~1 mV (Fig. 7a). Administration of DIDS elicited a negative shift in the V_m of ~5 mV, presumably due to the blockade of endogenous conductance. In the continued presence of DIDS, a second exposure to CO_2/HCO_3^- caused no further hyperpolarization. After the removal of DIDS, which was present for <50 s, a third exposure to CO_2/HCO_3^- again elicited a hyperpolarization larger than the first. We made similar observations for two other oocytes expressing construct O.

For the oocyte expressing construct T (Fig. 7c), the first and third CO_2/HCO_3^--induced V_m changes were larger than for construct O and more sustained. These changes were typical of three oocytes.

In the control oocyte injected with H_2O (Fig. 7c), we observed no hyperpolarizations during the first two applications of CO_2/HCO_3^-. After the removal of DIDS, the third application of CO_2/HCO_3^- elicited a slight, transient CO_2/HCO_3^--induced hyperpolarization that was typical of three oocytes. This slight hyperpolarization during the post-DIDS CO_2/HCO_3^- pulse appears to be common to all three oocyte groups (O, T, H_2O) and presumably represents an endogenous conductance that arises after pretreatment with DIDS.

In summary, the data in Fig. 7 demonstrate that, for both constructs O and T, the small CO_2/HCO_3^--induced hyperpolarizations are blocked by DIDS, indicating that they are mediated by the chimeric transporters.

Membrane Expression of Transporters

We have demonstrated that simultaneously replacing TM6 and TM12 severely reduces the functional expression of the transporter. The reduced functional expression reflects some combination of reduced transporter activity and a reduced number of transporters at the cell surface. We performed biotinylation assays to compare the surface-membrane expression of wt NBCe1-A with that of constructs O and T, the two chimeras that yielded the small transient hyperpolarizations upon switching the perfusing solution from ND96 to CO_2/HCO_3^-. As shown in Fig. 8a, b, compared to oocytes expressing wt NBCe1-A, those expressing constructs O and T had extremely low NBC protein abundance in the plasma membrane. The background signal of membrane preparations from nonbiotinylated oocytes expressing construct O or T was substantially less than that from biotinylated oocytes at these long exposures (data not shown).

We further examined the total transporter protein level by Western blotting with the whole lysate of *Xenopus* oocytes. Figure 8c shows that the total protein levels of construct O and

construct T are less than that of wt NBCe1-A. Moreover, the densitometric analysis in Fig. 8d shows that the total protein levels of constructs O and T are ~50% and ~65%, respectively, that of wt NBCe1-A, indicating that the reduction in total construct O and T protein relative to wt NBCe1-A is far less than the reduction in surface abundance.

Note that the molecular weight of the band in the wt NBCe1-A total protein lane (indicated by the arrow in Fig. 8c) is similar to that of the biotinylated band in Fig. 8a (also indicated by an arrow), which represents the fraction localized on the plasma membrane. This band represents the mature glycosylated form of NBCe1 (Chen et al. 2011) and is the major species present in the plasma membrane, consistent with previously published deglycosylation assays (Chen et al. 2011). The lower–molecular weight bands in Fig. 8c (indicated by an arrowhead) represent the immature or nonglycosylated forms of the transporter that predominantly resides in cytosolic compartments and is the major species present in the total lysate. Importantly, the very small fraction of constructs O and T that is expressed at the cell surface also has a molecular weight consistent with that of mature glycosylated NBCe1-A.

Collectively, the data in Fig. 8 suggest that the predominant effect of the dual replacement of TM6 and TM12 of NBCe1 with the comparable portions of NBCn1 severely reduces the presence of the chimeric transporters at the plasma membrane.

Discussion

Topology Model of NCBT

The consensus is that the TMD of NCBTs contains 14 TM segments. No fine structures are available for members of the SLC4 family; and the topology, particularly the back half of TMD, of these transporters is a subject of debate. In the topology model proposed by Romero et al. (2004)—in turn based on the AE1 model by Zhu et al. (2003)—13 of these 14 TMs are helices, whereas TM12 is an extended structure, extending from the extracellular to the intracellular side. This Romero model is the basis of all folding diagrams presented in this investigation as well as the previous one (Chen et al. 2011). In a more recent study, Zhu et al. (2010) proposed that the TMD of NBCe1 contains 14 TM helices. The sequence assignments of Zhu et al. (2010) from Nt through TM9 are basically consistent with the Romero model. A major difference in the model of Zhu et al. (2010) is that the segment from Val^{798} to Lys^{812}, which in the Romero model (2004) is a portion of a loop between TM9 and TM10, forms a Tm helix from the extracellular to the intracellular side. Therefore, the orientations of TM11 and TM12 in the Zhu model are inverted compared to the corresponding TM10 and TM11 in the Romero model. As a result, the extended structure (TM12) in the Romero model—identified as a key element in the present study—would, in the Zhu model, become the intracellular half of TM12, the sixth intracellular loop (IL6) and the intracellular half of TM13.

Electrogenicity of Chimeras

In the previous study, we demonstrated that the fourth extracellular loop—the sequence assignment for which is virtually identical in the Romero and Zhu models—plays a critical

role in determining the electrogenicity of NBCe1. In the present study, we made eight additional chimeras of human NBCe1-A and human NBCn1-A, all of which include EL4 of NBCe1. Consistent with our previous study, we find that all eight new chimeras have a CO_2/HCO_3^--induced ΔV_m, which is significantly different from that of H_2O-injected oocytes. In other words, they all appear to have a significant electrogenic component to their cotransport activity. Note that we cannot rule out the possibility that an electrically silent component exists in parallel with the electrogenic component.

Our previous article (Chen et al. 2011) showed that pairing EL5-Ct of NBCn1 with TM9 (construct F), TM8 (construct L) or TM7 (construct J) yields good functional expression. In the present series of chimeras, it is only the combination of EL5-Ct of NBCn1 with TM6 (construct O) that is problematic. Viewed from the opposite perspective, the present report shows that pairing the TM6 of NBCn1 with any of five other downstream elements from NBCn1—EL5 (construct Q), TM10 (construct R), TM11 (construct S), TM13-EL6 (construct U) and TM14 (construct V)—yields constructs with reasonably robust functional expression. It is specifically the combination of TM6 with TM12 from NBCn1 (construct T) that is problematic.

Our biotinylation data (Fig. 8a, b) show that, compared to wt NBCe1-A, the protein abundance of constructs O and T at the cell surface is substantially reduced. Nevertheless, when we switched from ND96 to CO_2/HCO_3^- in our electrophysiologic experiments, the oocytes expressing construct O or T consistently showed a small, abrupt hyperpolarization, which was not observed in oocytes injected with H_2O or expressing the electroneutral NBCn1 (for NBCn1, see Chen et al. 2011). Moreover, treatment with DIDS abolished these small hyperpolarizations (Fig. 7). Together, these observations are consistent with the notion that, although very low abundance of constructs O and T is present in the plasma membrane, they have at least a partial electrogenic character. Our data are not sufficiently quantitative to judge whether the per molecule (or intrinsic) acid-extrusion rates of these constructs are approximately normal.

Surface Expression of Chimeras

Analysis of the total transporter expression in *Xenopus* oocyte whole-cell lysate (Fig. 8c) indicates that the total protein levels of constructs O and T are modestly reduced compared to wt NBCe1-A and their mature glycosylated forms are barely detectable in this fraction. However, the reduction in total transporter expression compared to wt is far less than the reduction in biotinylated O and T detected at the surface relative to wt (Fig. 8b). The molecular weights of the construct O and T bands in the biotinylated fractions (Fig. 8a, b) are consistent with the size of mature glycosylated NBCe1-A. Therefore, the main cause of the functional impairment of NCBT chimeras with the TM6 and TM12 of NBCe1-A replaced by those from NBCn1 is to reduce the plasma membrane abundance of mature glycosylated, functional transporters. The molecular masses of O and T indicate that these proteins are mainly intact, providing no evidence of reduced protein stability. The presence of large amounts of immature or nonglycosylated protein is consistent with retention of the chimeras in intracellular compartments (e.g., ER, Golgi) rather than enhanced retrieval of the proteins from the plasma membrane.

It is interesting that simultaneous replacement of the putative TM6 and TM12 has such a great impact on the plasma membrane abundance of the transporter. If the topology of the NBCe1-A more closely follows that proposed by Zhu et al. (2010) than that by Romero et al. (2004), it is possible that the creation of constructs O and T has disrupted trafficking information predicted to reside in the cytoplasmic domains (in particular IL5, IL6 and the Ct). The region that we refer to as "TM12" contains motifs that, if exposed to the cytosol, could influence the trafficking of the transporter through intracellular organelles on its way to the surface. We expect SLC4 transporters—like other transporters and ion channels expressed at the plasma membrane, after folding and assembly—to enter the transitional ER. There, the SLC4 proteins would associate with Sec24 isoforms (A, B, C and D) that recognize distinct ER exit codes in cargo proteins and participate in the formation of coat protein complex II (COPII) export vesicles (Russell and Stagg 2010; Farhan et al. 2007; Srinivasan et al. 2011; Fernández-Sanchez et al. 2008). Impairing the association of the Sec proteins with plasma membrane proteins severely disrupts subsequent surface expression. The replacement of NBCe1-A TM12 with NBCn1 TM12 removes two putative ER exit codes (Mancias and Goldberg 2008; Wendeler et al. 2007) and introduces a YXXØ internalization motif that is not present in NBCe1-A (Bonifacino and Traub 2003). However, the differences in the TM12 region alone cannot explain the surface-expression deficits of constructs O and T because construct G (the only other construct possessing the NBCn1 TM12) functions almost as well as wt NBCe1-A.

The difference between construct G (with almost normal function) and construct O (barely expressed at the surface) is the presence of TM6 from NBCn1 in construct O. Although no refined crystal structure exists for an SLC4 protein, recently the structure of an SLC23 family member, the 14-transmembrane-segment *Escherichia coli* uracil/H^+ symporter UraA, was reported at a resolution of 2.8 Å (Lu et al. 2011). UraA possesses its own novel fold, but like other transporter families with solved structures, the UraA protomer is similarly formed by two inverted structural repeats, in this case TM1–7 and TM8–14 (Abramson and Wright 2009). Most interestingly, the hydropathic plot of UraA aligns well with that of NBCe1. TM5 and TM12 of UraA are at the center of a gating unit, which also contains TM6, TM7, TM13 and TM14. Let us hypothesize that NCBT structures adopt a 14-TM, UraA-like fold in which what we call "TM6" of NBCe1 (analogous to TM6 of UraA) is juxtaposed to what we call "TM12" of NBCe1 (analogous to TM12 of UraA). If true, it is reasonable to suggest that proper surface expression requires that the TM6/TM12 dihelical unit—if contributed by TMs of the same transporter type—be surrounded by gating-unit TMs (i.e., TM5 and TM7) that are also contributed by the same transporter type. According to the UraA model, what chimeras O and T have in common is a TM6/TM12 dihelical unit contributed by NBCn1 and adjacent gating-unit TMs contributed by NBCe1.

It is also constructive to consider NBCe1-A residue R881, which is highly conserved among members of the SLC4 family, with the exception of NBCe2. In humans, the mutation R881C causes severe proximal-type renal tubule acidosis (Horita et al. 2005). The mutation does not reduce the activity of NBCe1-A but does decrease the surface expression of NBCe1 transporters when expressed in *Xenopus* oocytes and causes retention in the ER when transiently expressed in Madin-Darby canine kidney cells (Toye et al. 2006). The proposed

location of the R881 is at the interface between the plasma membrane and cytosol, within TM12. If NCBT structures approximate a UraA-like fold, then R881 on TM12 would be near the cytosolic end of TM6.

In conclusion, the present study is consistent with the hypothesis that EL4 is necessary for the electrogenicity of NBCe1. In addition, simultaneous switching of the putative TM6 and TM12 of NBCe1 for those from NBCn1 severely impairs the expression of the transporter at the plasma membrane. We hypothesize that TM6 and TM12 are closely associated and part of a functional unit.

Acknowledgments

We are thankful to Dr. Mark D. Parker for his helpful discussions. This work was supported by NIH grants DK30344 and NS18400 to W. F. B. L.-M. C. was supported by grant 31000517 from the National Natural Science Foundation of China (NSFC). X. Q. was supported by grants 09POST2060873 and 11POST7670014 from the American Heart Association. Y. L. was supported by grant 30900513 from the NSFC. W. F. B. gratefully acknowledges the support of the Myers/Scarpa endowed chair.

References

Abramson J, Wright EM. Structure and function of Na^+-symporters with inverted repeats. Curr Opin Struct Biol. 2009; 19:425–432. [PubMed: 19631523]

Ahmed S, Thomas G, Ghoussaini M, et al. Newly discovered breast cancer susceptibility loci on 3p24 and 17q23.2. Nat Genet. 2009; 41:585–590. [PubMed: 19330027]

Antoniou AC, Beesley J, McGuffog L, et al. Common breast cancer susceptibility alleles and the risk of breast cancer for BRCA1 and BRCA2 mutation carriers: implications for risk prediction. Cancer Res. 2010; 70:9742–9754. [PubMed: 21118973]

Boedtkjer E, Praetorius J, Matchkov VV, Stankevicius E, Mogensen S, Füchtbauer AC, Simonsen U, Fuchtbauer EM, Aalkjaer C. Disruption of Na^+, HCO_3^- cotransporter NBCn1 (slc4a7) inhibits NO-mediated vasorelaxation, smooth muscle Ca^{2+} sensitivity, and hypertension development in mice. Circulation. 2011; 124:1819–1829. [PubMed: 21947296]

Bok D, Galbraith G, Lopez I, et al. Blindness and auditory impairment caused by loss of the sodium bicarbonate cotransporter NBC3. Nat Genet. 2003; 34:313–319. [PubMed: 12808454]

Bonifacino JS, Traub LM. Signals for sorting of transmembrane proteins to endosomes and lysosomes. Annu Rev Biochem. 2003; 72:395–447. [PubMed: 12651740]

Boron WF, Chen L, Parker MD. Modular structure of sodium-coupled bicarbonate transporters. J Exp Biol. 2009; 212:1697–1706. [PubMed: 19448079]

Bouyer P, Sakai H, Itokawa T, Kawano T, Fulton CM, Boron WF, Insogna KL. Colony-stimulating factor-1 increases osteoclast intracellular pH and promotes survival via the electroneutral Na/HCO_3 cotransporter NBCn1. Endocrinology. 2007; 148:831–840. [PubMed: 17068143]

Chen LM, Liu Y, Boron WF. Role of an extracellular loop in determining the stoichiometry of Na/HCO_3 cotransporters. J Physiol. 2011; 589:877–890. [PubMed: 21224233]

Choi I, Aalkjaer C, Boulpaep EL, Boron WF. An electroneutral sodium/bicarbonate cotransporter NBCn1 and associated sodium channel. Nature. 2000; 405:571–575. [PubMed: 10850716]

Choi I, Yang HS, Boron WF. The electrogenicity of the rat sodium-bicarbonate cotransporter NBCe1 requires interactions among transmembrane segments of the transporter. J Physiol. 2007; 578:131–142. [PubMed: 17038436]

De Giusti VC, Garciarena CD, Aiello EA. Role of reactive oxygen species (ROS) in angiotensin II-induced stimulation of the cardiac Na^+/HCO_3^- cotransport. J Mol Cell Cardiol. 2009; 47:716–722. [PubMed: 19646989]

De Giusti VC, Orlowski A, Aiello EA. Angiotensin II inhibits the electrogenic Na^+/HCO_3^- cotransport of cat cardiac myocytes. J Mol Cell Cardiol. 2010; 49:812–818. [PubMed: 20692267]

Ehret GB, Munroe PB, Rice KM, et al. Genetic variants in novel pathways influence blood pressure and cardiovascular disease risk. Nature. 2011; 478:103–109. [PubMed: 21909115]

Farhan H, Reiterer V, Korkhov VM, Schmid JA, Freissmuth M, Sitte HH. Concentrative export from the endoplasmic reticulum of the γ-aminobutyric acid transporter 1 requires binding to SEC24D. J Biol Chem. 2007; 282:7679–7689. [PubMed: 17210573]

Fernández-Sánchez E, Díez-Guerra FJ, Cubelos B, Giménez C, Zafra F. Mechanisms of endoplasmic-reticulum export of glycine transporter-1 (GLYT1). Biochem J. 2008; 409:669–681. [PubMed: 17919119]

Grichtchenko II, Choi I, Zhong X, Bray-Ward P, Russell JM, Boron WF. Cloning, characterization, and chromosomal mapping of a human electroneutral Na^+-driven Cl-HCO_3 exchanger. J Biol Chem. 2001; 276:8358–8363. [PubMed: 11133997]

Horita S, Yamada H, Inatomi J, Moriyama N, Sekine T, Igarashi T, Endo Y, Dasouki M, Ekim M, Al Gazali L, Shimadzu M, Seki G, Fujita T. Functional analysis of NBC1 mutants associated with proximal renal tubular acidosis and ocular abnormalities. J Am Soc Nephrol. 2005; 16:2270–2278. [PubMed: 15930088]

Ishiguro H, Walther D, Arinami T, Uhl GR. Variation in a bicarbonate co-transporter gene family member SLC4A7 is associated with propensity to addictions: a study using fine-mapping and three samples. Addiction. 2007; 102:1320–1325. [PubMed: 17624982]

Khandoudi N, Albadine J, Robert P, Krief S, Berrebi-Bertrand I, Martin X, Bevensee MO, Boron WF, Bril A. Inhibition of the cardiac electrogenic sodium bicarbonate cotransporter reduces ischemic injury. Cardiovasc Res. 2001; 52:387–396. [PubMed: 11738055]

Kumar S, Flacke JP, Kostin S, Appukuttan A, Reusch HP, Ladilov Y. SLC4A7 sodium bicarbonate co-transporter controls mitochondrial apoptosis in ischaemic coronary endothelial cells. Cardiovasc Res. 2010; 89:392–400. [PubMed: 20962104]

Lacruz RS, Nanci A, White SN, Wen X, Wang H, Zalzal SF, Luong VQ, Schuetter VL, Conti PS, Kurtz I, Paine ML. The sodium bicarbonate cotransporter (NBCe1) is essential for normal development of mouse dentition. J Biol Chem. 2010; 285:24432–24438. [PubMed: 20529845]

Lauritzen G, Jensen MB, Boedtkjer E, Dybboe R, Aalkjaer C, Nylandsted J, Pedersen SF. NBCn1 and NHE1 expression and activity in ΔNErbB2 receptor-expressing MCF-7 breast cancer cells: contributions to pHi regulation and chemotherapy resistance. Exp Cell Res. 2010; 316:2538–2553. [PubMed: 20542029]

Liu Y, Xu JY, Wang DK, Wang L, Chen LM. Cloning and identification of two novel NBCe1 splice variants from mouse reproductive tract tissues: a comparative study of NCBT genes. Genomics. 2011; 98:112–119. [PubMed: 21600280]

Lu J, Boron WF. The reversible and irreversible interactions of DIDS with the human electrogenic Na/HCO_3 cotransporter (hNBCe1-A): importance of K558, K559 and K562 within the KKMIK motif of transmembrane segment 5. Am J Physiol Cell Physiol. 2007; 292:C1787–C1798. [PubMed: 17251325]

Lu F, Li S, Jiang Y, Jiang J, Fan H, Lu G, Deng D, Dang S, Zhang X, Wang J, Yan N. Structure and mechanism of the uracil transporter UraA. Nature. 2011; 472:243–246. [PubMed: 21423164]

Mancias JD, Goldberg J. Structural basis of cargo membrane protein discrimination by the human COPII coat machinery. EMBO J. 2008; 27:2918–2928. [PubMed: 18843296]

Parker MD, Musa-Aziz R, Rojas JD, Choi I, Daly CM, Boron WF. Characterization of human SLC4A10 as an electroneutral Na/HCO_3 cotransporter (NBCn2) with Cl^- self-exchange activity. J Biol Chem. 2008; 283:12777–12788. [PubMed: 18319254]

Pushkin A, Abuladze N, Lee I, Newman D, Hwang J, Kurtz I. Cloning, tissue distribution, genomic organization, and functional characterization of NBC3, a new member of the sodium bicarbonate cotransporter family. J Biol Chem. 1999; 274:16569–16575. [PubMed: 10347222]

Riihonen R, Nielsen S, Vaananen HK, Laitala-Leinonen T, Kwon TH. Degradation of hydroxyapatite in vivo and in vitro requires osteoclastic sodium-bicarbonate co-transporter NBCn1. Matrix Biol. 2010; 29:287–294. [PubMed: 20079835]

Romero MF, Hediger MA, Boulpaep EL, Boron WF. Expression cloning and characterization of a renal electrogenic Na^+/HCO_3^- cotransporter. Nature. 1997; 387:409–413. [PubMed: 9163427]

Romero MF, Fulton CM, Boron WF. The SLC4 family of HCO_3^- transporters. Pflugers Arch. 2004; 447:495–509. [PubMed: 14722772]

Russell C, Stagg SM. New insights into the structural mechanisms of the COPII coat. Traffic. 2010; 11:303–310. [PubMed: 20070605]

Sassani P, Pushkin A, Gross E, Gomer A, Abuladze N, Dukkipati R, Carpenito G, Kurtz I. Functional characterization of NBC4: a new electrogenic sodium-bicarbonate cotransporter. Am J Physiol Cell Physiol. 2002; 282:C408–C416. [PubMed: 11788353]

Srinivasan R, Pantoja R, Moss FJ, Mackey ED, Son CD, Miwa J, Lester HA. Nicotine up-regulates α4β2 nicotinic receptors and ER exit sites via stoichiometry-dependent chaperoning. J Gen Physiol. 2011; 137:59–79. [PubMed: 21187334]

Suzuki M, Van Paesschen W, Stalmans I, et al. Defective membrane expression of the Na^+-HCO_3^- cotransporter NBCe1 is associated with familial migraine. Proc Natl Acad Sci USA. 2010; 107:15963–15968. [PubMed: 20798035]

Toye AM, Parker MD, Daly CM, Lu J, Virkki LV, Pelletier MF, Boron WF. The human NBCe1-A mutant R881C, associated with proximal renal tubular acidosis, retains function but is mistargeted in polarized renal epithelia. Am J Physiol Cell Physiol. 2006; 291:C788–C801. [PubMed: 16707554]

Virkki LV, Wilson DA, Vaughan-Jones RD, Boron WF. Functional characterization of human NBC4 as an electrogenic Na^+-HCO_3^- cotransporter (NBCe2). Am J Physiol Cell Physiol. 2002; 282:C1278–C1289. [PubMed: 11997242]

Wang CZ, Yano H, Nagashima K, Seino S. The Na^+-driven Cl^-/HCO_3^- exchanger: cloning, tissue distribution, and functional characterization. J Biol Chem. 2000; 275:35486–35490. [PubMed: 10993873]

Wendeler MW, Paccaud JP, Hauri HP. Role of Sec24 isoforms in selective export of membrane proteins from the endoplasmic reticulum. EMBO Rep. 2007; 8:258–264. [PubMed: 17255961]

Zhu Q, Lee DW, Casey JR. Novel topology in C-terminal region of the human plasma membrane anion exchanger, AE1. J Biol Chem. 2003; 278:3112–3120. [PubMed: 12446737]

Zhu Q, Kao L, Azimov R, Abuladze N, Newman D, Pushkin A, Liu W, Chang C, Kurtz I. Structural and functional characterization of the C-terminal transmembrane region of NBCe1-A. J Biol Chem. 2010; 285:37178–37187. [PubMed: 20837482]

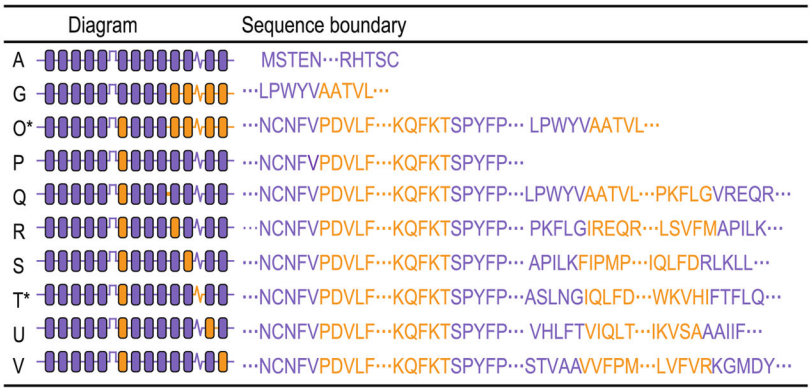

Fig. 1.

Diagrams and sequence boundaries of constructs. Regions that contributed human NBCe1-A are in *violet*, whereas regions that contributed by human NBCn1 are in *orange*

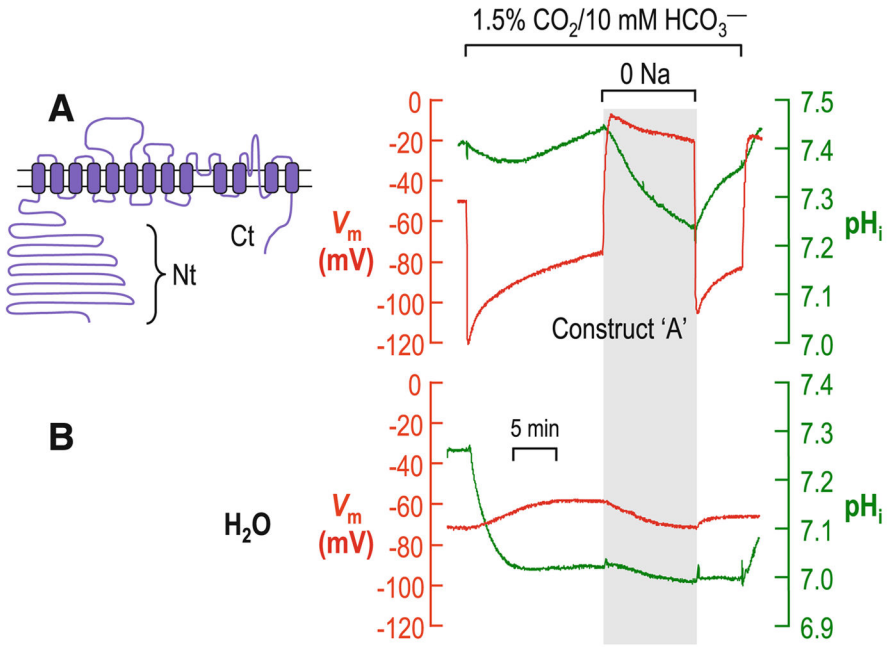

Fig. 2.

Typical recordings of pH_i (*green*) and V_m (*red*, in mV). **a** Oocyte expressing human NBCe1-A (construct A). **b** Control oocyte injected with H_2O. The oocyte was first exposed to ND96 (CO_2/HCO_3^--free) solution, and then to 1.5% CO_2/10 mM HCO_3^- for 15 min, all at an extracellular pH of 7.50. Extracellular Na^+ was temporarily replaced with *N*-methyl-D-glucamine for 10 min, and returned for 5 min in the continued presence of CO_2/HCO_3^-

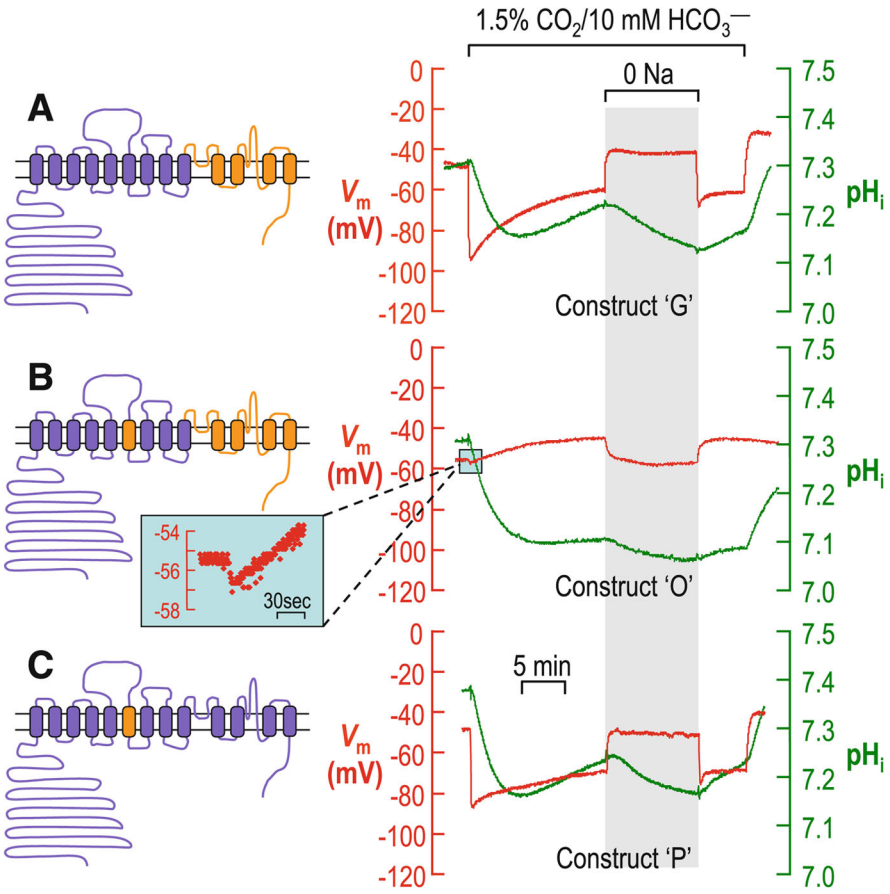

Fig. 3.

Typical recordings of pH_i (*green*) and V_m (*red*, in mV) of oocytes expressing chimeric transporters. **a** Construct G. **b** Construct O. **c** Construct P. The experimental protocols are the same as for Fig. 2. The sequence boundaries of the constructs are provided in Fig. 1. *Inset* in *b* shows, in a magnified scale, the small hyperpolarization upon the switch from the ND96 to the CO_2/HCO_3^- solution

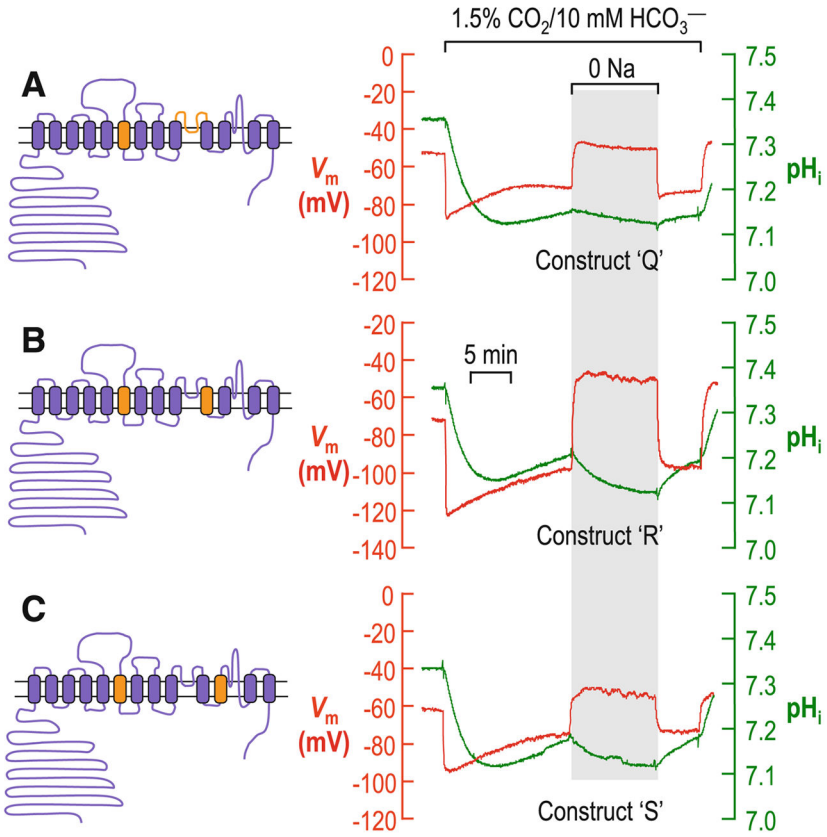

Fig. 4.

Typical recordings of pH_i (*green*) and V_m (*red*, in mV) of oocytes expressing chimeric transporters. **a** Construct Q. **b** Construct R. **c** Construct S. The experimental protocols are the same as for Figs. 2 and 3. The sequence boundaries of the constructs are provided in Fig. 1

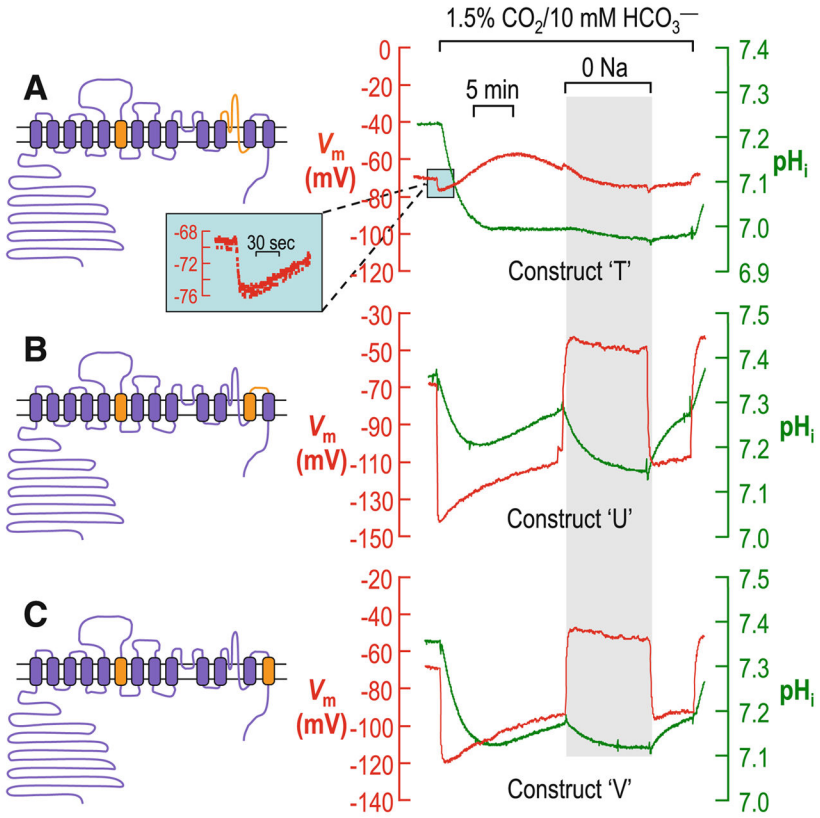

Fig. 5.

Typical recordings of pH_i (*green*) and V_m (*red*, in mV) of oocytes expressing chimeric transporters. **a** Construct T. **b** Construct U. **c** Construct V. The experimental protocols are the same as for Figs. 2, 3, and 4. The sequence boundaries of the constructs are provided in Fig. 1. *Inset* in *a* shows, in magnified scale, the small hyperpolarization upon the switch from the ND96 to the CO_2/HCO_3^- solution

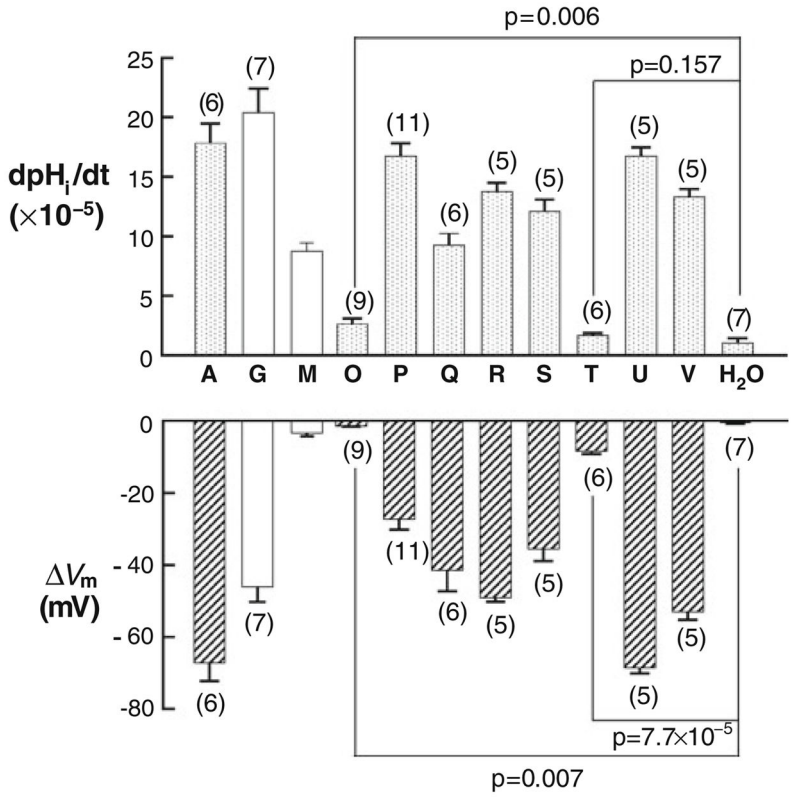

Fig. 6.

Summary of pH_i recovery rates and maximum V_m changes of oocytes. Bars for constructs G and M are reproduced from Chen et al. (2011). All data for other bars are new and were collected from experiments like those shown in Figs. 2, 3, 4, and 5. dpH_i/dt represents the maximal pH_i recovery rates of oocytes after the initial CO_2-induced acidification. ΔV_m represents the maximum instantaneous V_m changes upon the switch to 1.5% CO_2/10 mM HCO_3^- during the first CO_2/HCO_3^- pulse. Data are presented as mean ± SEM. Welch's unpaired *t*-test was performed to examine if the dpH_i/dt or ΔV_m of oocytes expressing transporters was significantly different from that of control oocytes injected with H_2O. The difference was considered significant if $P \leq 0.01$

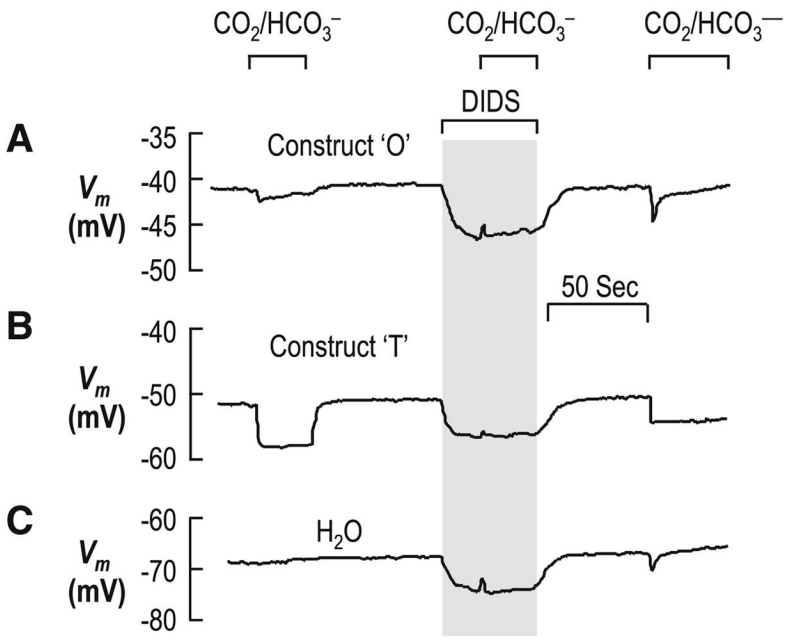

Fig. 7.

Effect of DIDS on CO_2/HCO_3^--induced changes in V_m of *Xenopus* oocytes. **a** Construct O. **b** Construct T. **c** Control oocyte injected with H_2O. The extracellular solution was alternated between ND96 (CO_2/HCO_3^--free) solution and 1.5% CO_2/10 mM HCO_3^-, all at an extracellular pH of 7.50. All solutions were supplemented with 0.2% BSA if 400 μM DIDS was not present. Shown here are V_m traces representative of three independent experiments for each case

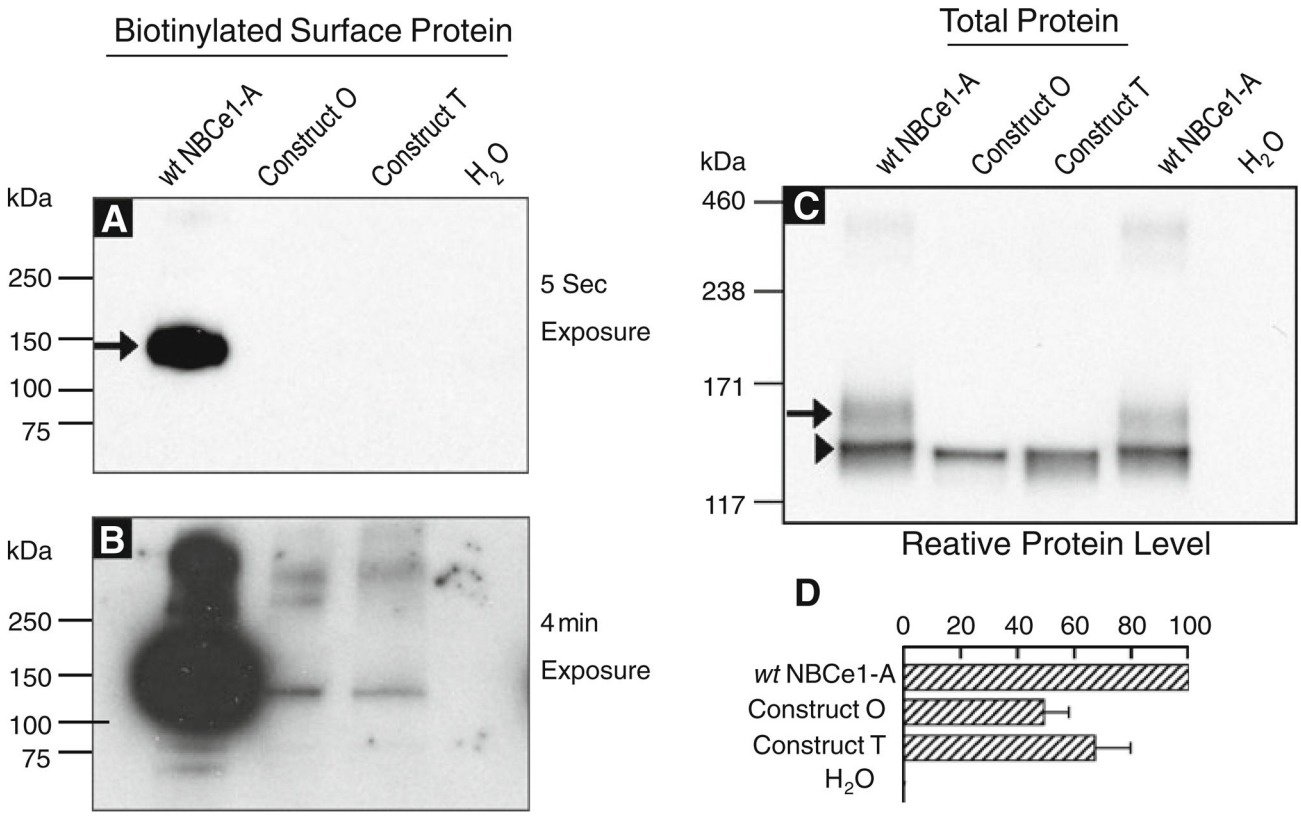

Fig. 8.

Protein expression of transporters in expressed *Xenopus* oocytes. **a** Surface expression of transporter protein, detected with short exposure. **b** Longer exposure from the same blot as in **a. c** Total protein level of transporters expressed in *Xenopus* oocytes. **d** Summary of densitometric analysis for total protein levels. The surface protein was obtained using a biotinylation approach. In each lane, the same amount of surface protein or total protein was loaded and resolved by SDS-PAGE, then analyzed by Western blot. *Arrows* in **a** and **c** indicate the glycosylated form of NBCe1-A, whereas *arrowhead* in c indicates the immature or nonglycosylated form of the transporter. Densitometric analysis was performed for three independent blots like that shown in **c**. The density of each lane was normalized to that of wt NBCe1-A, which was arbitrarily set to 100